The Plant Cell, Vol. 7, 2101–2114, December 1995

Tobacco Mosaic Virus Movement Protein Associates with the Cytoskeleton in Tobacco Cells

B. Gail McLean, John Zupan, and Patricia C. Zambryski[1]

Department of Plant Biology, University of California–Berkeley, Berkeley, California 94720-3102

Tobacco mosaic virus movement protein P30 complexes with genomic viral RNA for transport through plasmodesmata, the plant intercellular connections. Although most research with P30 focuses on its targeting to and gating of plasmodesmata, the mechanisms of P30 intracellular movement to plasmodesmata have not been defined. To examine P30 intracellular localization, we used tobacco protoplasts, which lack plasmodesmata, for transfection with plasmids carrying P30 coding sequences under a constitutive promoter and for infection with tobacco mosaic virus particles. In both systems, P30 appears as filaments that colocalize primarily with microtubules. To a lesser extent, P30 filaments colocalize with actin filaments, and in vitro experiments suggested that P30 can bind directly to actin and tubulin. This association of P30 with cytoskeletal elements may play a critical role in intracellular transport of the P30-viral RNA complex through the cytoplasm to and possibly through plasmodesmata.

INTRODUCTION

To establish a systemic infection, plant viruses must move from the infection site to the rest of the plant. For many plant viruses, a virus-encoded product, the movement protein, actively potentiates viral cell-to-cell spread through plasmodesmata, the cytoplasmic bridges that function as intercellular connections (Gibbs, 1976; reviewed in Deom et al., 1992; Citovsky and Zambryski, 1993; McLean et al., 1993; Lucas and Gilbertson, 1994). One of the most extensively studied viral movement proteins is the P30 protein of tobacco mosaic virus (TMV), a relatively simple, positive sense, single-stranded RNA virus. P30 (also termed TMV MP) is proposed to form a complex with the genomic TMV RNA, to target this protein–nucleic acid complex to plasmodesmata, and to transport it through the now-enlarged, open plasmodesmata (Citovsky and Zambryski, 1991). Virtually all research on P30-mediated cell–cell movement focuses on the interaction, that is, targeting and gating, with plasmodesmata. Yet, synthesis of P30, replication of TMV RNA, and presumably, formation of the P30–viral RNA complex all occur in the host cell cytoplasm. Therefore, the P30–RNA complex must move through the cytoplasm to the plasmodesmata.

The mechanism by which P30 moves intracellularly to reach the plasmodesmata is not known. Since the protein content and organized nature of the cytoplasm probably restrict diffusion of large molecular complexes, such as protein–nucleic acid complexes (Luby-Phelps, 1993, 1994), movement of the P30–RNA complex to plasmodesmata most likely is not by passive diffusion. Along these lines, numerous studies suggest that the cytoskeleton acts as a trafficking system for intracellular transport, translocating vesicles, organelles, protein, and even mRNA to specific cellular locations (Williamson, 1986; Vale, 1987; Dingwall, 1992; Singer, 1992; Wilhelm and Vale, 1993; Bassell et al., 1994; Hesketh, 1994). An intriguing possibility is that directional movement of the P30–RNA complex through the cytoplasm occurs on cytoskeletal components.

In a somewhat analogous situation, many animal viruses spread through the host cell by interacting with host cell cytoskeletal components. Specifically, the microtubule network appears to play an important role in viral protein trafficking and distribution in animal cells (Pasick et al., 1994). For example, the viral matrix protein of vesicular stomatitus virus associates with tubulin in vitro and in vivo; the in vitro data show that this viral protein can bind to both polymerized and unpolymerized tubulin (Melki et al., 1994). In sensory neurons, the transport of herpes simplex virus occurs in a plus–minus direction on microtubules, suggesting that directional transport of herpes simplex virus is mediated by a minus end–directed motor, such as cytoplasmic dynein (Topp et al., 1994).

Like the animal cytoskeleton, the plant cytoskeleton is composed of filamentous networks of actin, tubulin (microtubules), and intermediate filaments. Although the plant cytoskeleton and its components are not as well characterized as those in animals, experimental data and evolutionary conservation of the cytoskeletal proteins suggest that both the general mechanisms and the functions of the cytoskeleton are conserved between animals and plants (reviewed in Lloyd, 1982; Staiger and Lloyd, 1991; Shibaoka and Nagai, 1994). Thus, both plants and animals may use cytoskeletal filaments and motor proteins

[1] To whom correspondence should be addressed.

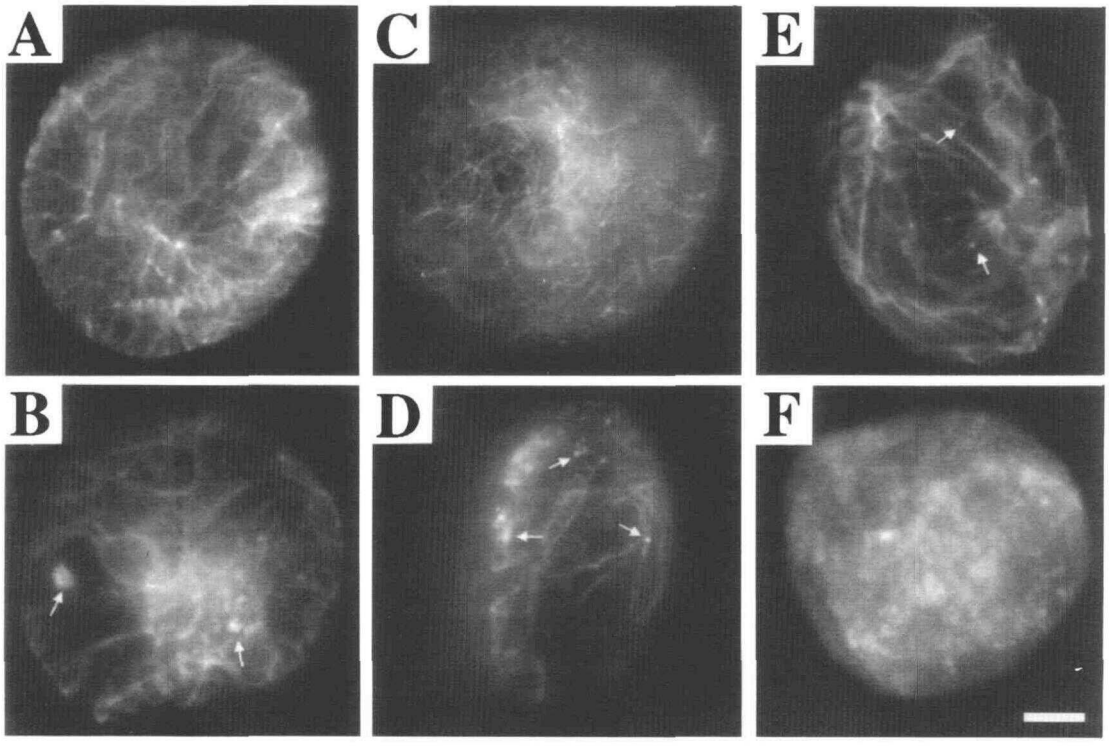

Figure 1. Filamentous Appearance of Transiently Expressed Wild-Type P30 in Tobacco Protoplasts.

P30 was detected by affinity-purified P30 polyclonal antibody and fluorescein-conjugated goat anti-rabbit secondary antibody. Arrows in **(B)**, **(D)**, and **(E)** denote P30 aggregates.

(A) to **(C)** P30 in aldehyde-fixed protoplasts.

(D) and **(E)** P30 in a detergent-permeabilized unfixed protoplasts.

(F) P30 sb-6 mutant (Citovsky et al., 1993) in an aldehyde-fixed protoplast.

Bar in **(F)** = 10 μm for **(A)** to **(F)**.

to move macromolecular complexes, such as ribonucleoprotein particles. In addition, evolutionary studies suggest that viruses act as scavengers, exploiting host cellular genes and processes and adapting them for the viruses' life cycle (Haseloff et al., 1984; Zimmern, 1988; Morozov et al., 1989; Citovsky, 1993; Koonin and Dolja, 1993). Hypothetically, the viral P30–RNA complexes may mimic ribonucleoprotein particles and use the cytoskeleton as a highway through the cytoplasm to the plasmodesmata.

To begin characterizing the process of P30 movement within and through the plant cell cytoplasm, we examined the intracellular localization of P30 in tobacco cells. P30 must be confined to a single cell for such studies. To prevent transport of P30 out of the cell, plasmodesmata need to be absent or nonfunctional (Deom et al., 1987; Meshi et al., 1987; Moser et al., 1988). Consequently, tobacco protoplasts were used. Protoplasts are an ideal system for studying intracellular localization of proteins. The protoplast itself is a single cell, and importantly, the process of removing the cell wall severs plasmodesmata. Thus, P30 is restricted to a single cell, allowing analysis of P30 in the cytoplasm before targeting to plasmodesmata. Here, we show that P30 forms a filamentous network that is coincident with the cytoskeleton in tobacco protoplasts.

RESULTS

Expression of P30 in Protoplasts

To examine expression of TMV P30 in tobacco protoplasts, the P30 coding region was cloned into pRTL2, a plant expression vector containing the cauliflower mosaic virus (CaMV) 35S promoter and the untranslated leader of tobacco etch virus (Restrepo et al., 1990). Consequently, P30 alone is produced in the cell, thus separating P30 expression from other TMV proteins. Protoplasts were prepared from tobacco cell suspension cultures, electroporated with plasmid DNA, and incubated 18 to 20 hr to allow the expression of the introduced DNA. P30 was detected by affinity-purified anti-P30 polyclonal antibodies, followed by fluorescein-conjugated secondary antibody. Fluorescence was not detected in untransfected protoplasts or with preimmune serum.

As shown in Figure 1, when expressed alone in protoplasts, P30 appears as a filamentous network reminiscent of the cytoskeleton in both fixed (Figures 1A to 1C) and unfixed (Figures 1D and 1E) protoplasts. The appearance of P30 varied from very dense, fine filaments (Figures 1A and 1C) to less

dense, thicker filaments (Figures 1B, 1D, and 1E), depending on the particular protoplast being examined. Protoplasts permeabilized or fixed without DMSO also showed both fine and thick filaments, indicating that the presence of DMSO did not cause bundling of the P30 filaments (data not shown). In some protoplasts, small aggregates of P30 could be seen associated with the P30 filaments. To confirm that the filamentous network results from a specific activity of P30 and not simply from its overexpression, a substitution mutant of P30, sb-6, was also transfected and expressed in tobacco protoplasts (Citovsky et al., 1993). Although wild-type P30, a tenacious single-stranded nucleic acid binding protein, binds both RNA and single-stranded DNA (Citovsky et al., 1990), sb-6 binds RNA but no longer binds single-stranded DNA; sb-6 also can be phosphorylated by the cell wall–associated kinase described in Citovsky et al. (1993). As shown in Figure 1F, sb-6 does not form the filamentous network typical of wild-type P30 in protoplasts but rather appears as more random aggregates in the cell.

To confirm that the localization of P30 in the transient assay reflected localization of virus-encoded P30, virus-infected protoplasts were examined. Protoplasts, prepared from tobacco suspension cells, were inoculated with TMV in the presence of polyethylene glycol (Maule et al., 1980) and incubated for 10 hr to allow expression of P30. Previous studies have shown that, in both inoculated tobacco protoplasts and infected cells of intact tobacco leaves, P30 accumulates to maximal amounts during the early stages of TMV infection (Kiberstis et al., 1983; Watanabe et al., 1984; Blum et al., 1989; Lehto et al., 1990). In an electron microscopy study, Meshi et al. (1992) found P30 near the nucleus in TMV-infected protoplasts; however, during later stages of virus infection (15 to 24 hr after inoculation), P30 was observed at confined areas in the cytoplasm. In our studies, fluorescence microscopy has been used because it permits gentler and potentially less disruptive fixation of P30-expressing cells.

P30 was detected with affinity-purified anti-P30 polyclonal antibodies followed by fluorescein-conjugated secondary

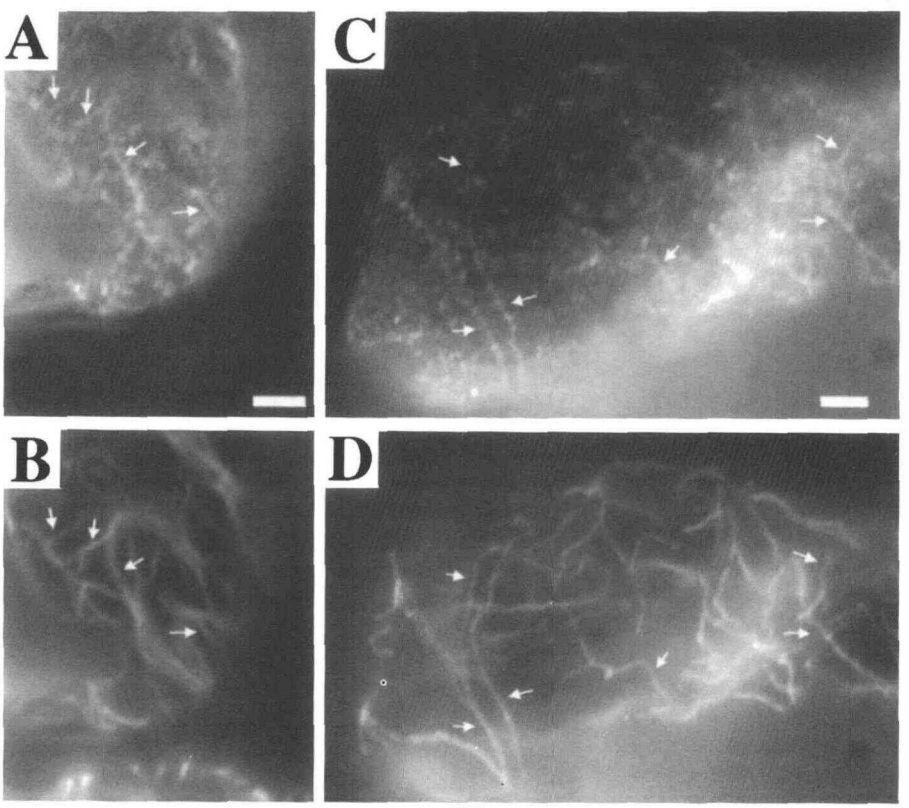

Figure 2. Association of P30 with Microtubules in TMV-Infected Protoplasts.

P30 was detected by affinity-purified P30 polyclonal antibody and fluorescein-conjugated goat anti–rabbit secondary antibody. Microtubules were detected by monoclonal tubulin antibody and rhodamine-conjugated goat anti–mouse secondary antibody. Arrows highlight areas showing colocalized P30 and microtubules.

(A) P30 in an aldehyde-fixed protoplast.

(B) Microtubules in the aldehyde-fixed protoplast shown in **(A)**.

(C) P30 in another aldehyde-fixed protoplast.

(D) Microtubules in the aldehyde-fixed protoplast shown in **(C)**.

Bar in **(A)** = 3.5 μm for **(A)** and **(B)**; bar in **(C)** = 3.1 μm for **(C)** and **(D)**.

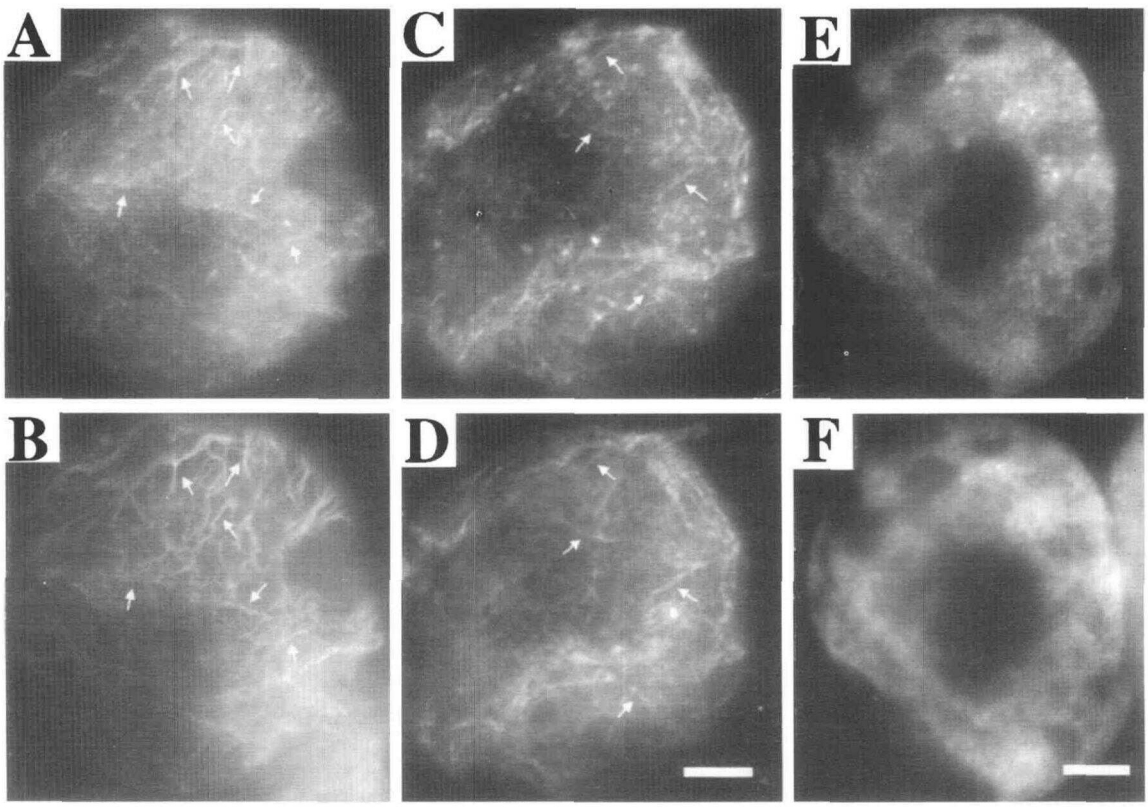

Figure 3. *Colocalization of P30 with Microtubules.*

Wild-type P30 was detected by affinity-purified P30 polyclonal antibody and fluorescein-conjugated goat anti–rabbit secondary antibody. Microtubules were detected by monoclonal tubulin antibody and rhodamine-conjugated goat anti–mouse secondary antibody. Arrows in **(A)** to **(D)** indicate colocalized P30 and microtubules.

(A) P30 in an aldehyde-fixed protoplast.

(B) Microtubules in the aldehyde-fixed protoplast shown in **(A)**.

(C) P30 in another aldehyde-fixed protoplast.

(D) Microtubules in the aldehyde-fixed protoplast shown in **(C)**.

(E) P30 in an aldehyde-fixed protoplast after incubation at 0°C to depolymerize microtubules.

(F) Microtubules in the aldehyde-fixed protoplast shown in **(E)** after incubation at 0°C.

Bar in **(D)** = 10 μm for **(A)** to **(D)**; bar in **(F)** = 10 μm for **(E)** and **(F)**.

antibody. Fluorescence was not detected in uninfected protoplasts or with preimmune serum. As shown in Figures 2A and 2C, P30 appears as filamentous structures and as distinct spots in protoplasts 10 hr after TMV infection. The presence of P30 spots as well as P30 filaments in virus-infected cells may have resulted from P30 interacting with other viral proteins. For instance, P30 may accumulate at regions of TMV replication and protein synthesis, in other words, near polyribosomes and the endoplasmic reticulum found in inclusion bodies that are typical of TMV-infected cells. As observed by fluorescence microscopy, the amount of P30 in virus-infected protoplasts was noticeably higher than in P30-transfected protoplasts, where P30 is expressed from a CaMV 35S promoter.

Since both virus-infected and P30-transfected protoplasts display filamentous P30, the localization of transiently expressed P30 appeared to mimic that of P30 during virus infection. This localization most likely represents a biological function of P30 because a genetically altered form of P30 that was transiently expressed at high levels failed to form filaments (Figure 1F). Thus, the P30 transient expression assay provides a simple system to study cytoplasmic regionalization of newly synthesized P30. Since TMV-infected protoplasts accumulate other virus-encoded proteins that potentially may interfere with P30 localization, the transient expression system was used to further characterize P30 expression in protoplasts.

Interaction of P30 with Microtubules and Actin Filaments

In virus-infected protoplasts and in transfected protoplasts expressing P30 alone, P30 produces a filamentous network. Since the organization of this P30 network resembles the plant

cytoskeleton, we examined the localization of P30 with the two major components of the plant cytoskeleton: microtubules and actin filaments. For studies comparing the possible colocalization of P30 filaments and microtubules, P30 was detected with affinity-purified antibodies and fluorescein-conjugated secondary antibody; microtubules were detected with a monoclonal anti-tubulin antibody and rhodamine-conjugated secondary antibody. Controls showed that rhodamine fluorescence did not contaminate the fluorescein signal; for example, protoplasts not expressing P30 but reacting with the tubulin antibody did not produce a signal in the fluorescein channel (compare lower portions of Figures 2A and 2B).

As demonstrated in Figures 2 and 3, a number of P30 filaments were observed to colocalize with microtubules in both virus-infected and P30-transfected cells (Figures 2A to 2D and Figures 3A to 3D). To confirm that the P30 interacts specifically with microtubules, transfected protoplasts were incubated at 0°C to depolymerize the microtubules before fixation; this cold treatment did not depolymerize the actin filaments (data not shown). P30 filaments that result from interaction with microtubules should be disrupted by the cold treatment, leading to loss or decreased number of filaments. Indeed, cold treatment had a dramatic effect on the P30 network, typically causing a large increase in P30 aggregates, with a concomitant decrease in P30 filaments (Figure 3E). Thus, the cold treatment that disrupted the microtubules (Figure 3F) also destroyed most of the P30 filaments. Although the breakdown of the microtubule network produced diffuse tubulin staining and shortened microtubules, the loss of P30 filaments resulted in aggregates or spots of P30. Interestingly, in some cold-treated protoplasts, a few P30 filaments remained after intact microtubules could no longer be detected (data not shown), suggesting that a subset of the P30 filaments did not associate with microtubules.

Since the other major component of the cytoskeleton, the actin filament network, was not disrupted by cold treatment, a potential interaction of P30 with the actin cytoskeleton was assayed. Again, P30 was detected with affinity-purified antibodies and fluorescein-conjugated secondary antibody. Actin was detected with rhodamine-phalloidin, which binds actin filaments. As noted previously, rhodamine fluorescence did not appear in the fluorescein channel. Figure 4 shows that some

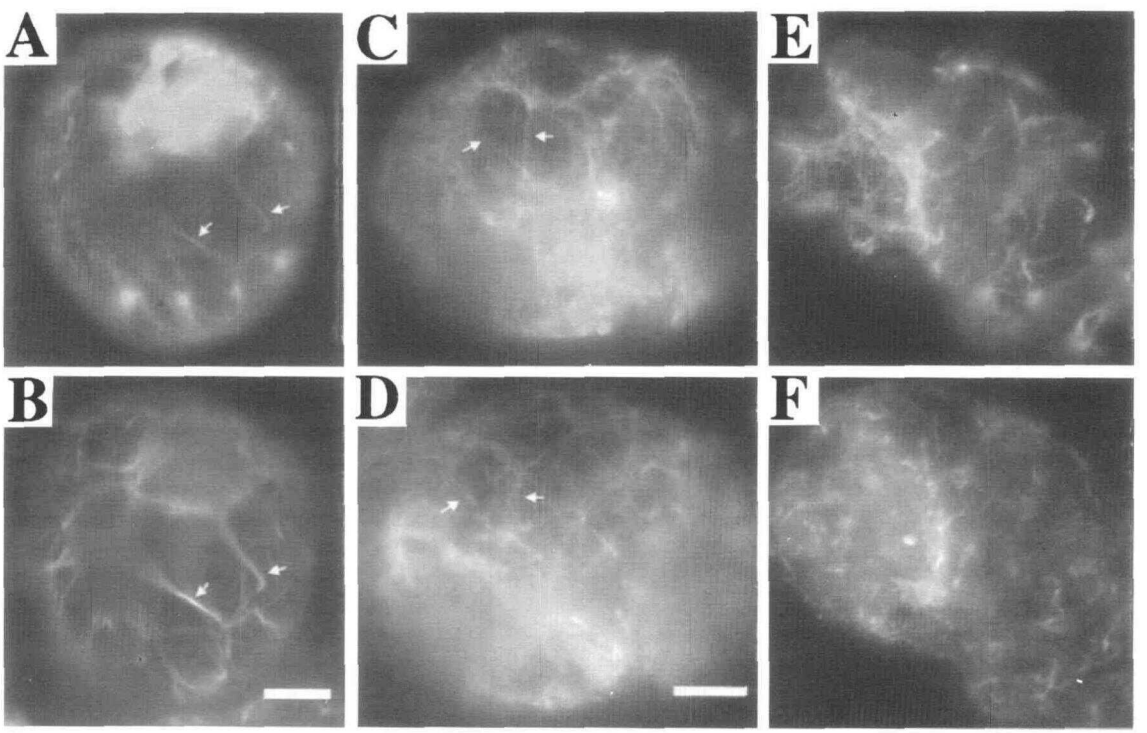

Figure 4. Colocalization of P30 with Actin Filaments.

Wild-type P30 was detected by affinity-purified P30 polyclonal antibody and fluorescein-conjugated goat anti–rabbit secondary antibody. Actin filaments were detected with rhodamine-conjugated phalloidin. Arrows in **(A)** to **(D)** denote colocalized P30 and actin filaments.

(A) P30 in an aldehyde-fixed protoplast. Note the association of P30 with the nucleus in this cell.

(B) Actin filaments in the aldehyde-fixed protoplast shown in **(A)**.

(C) P30 in another aldehyde-fixed protoplast.

(D) Actin filaments in the aldehyde-fixed protoplast shown in **(C)**.

(E) P30 in an aldehyde-fixed protoplast after pretreatment with cytochalasin D to disrupt actin filaments.

(F) Actin in the same aldehyde-fixed protoplast shown in **(E)** after pretreatment with cytochalasin D.

Bar in **(B)** = 10 μm for **(A)** and **(B)**; bar in **(D)** = 10 μm for **(C)** to **(F)**.

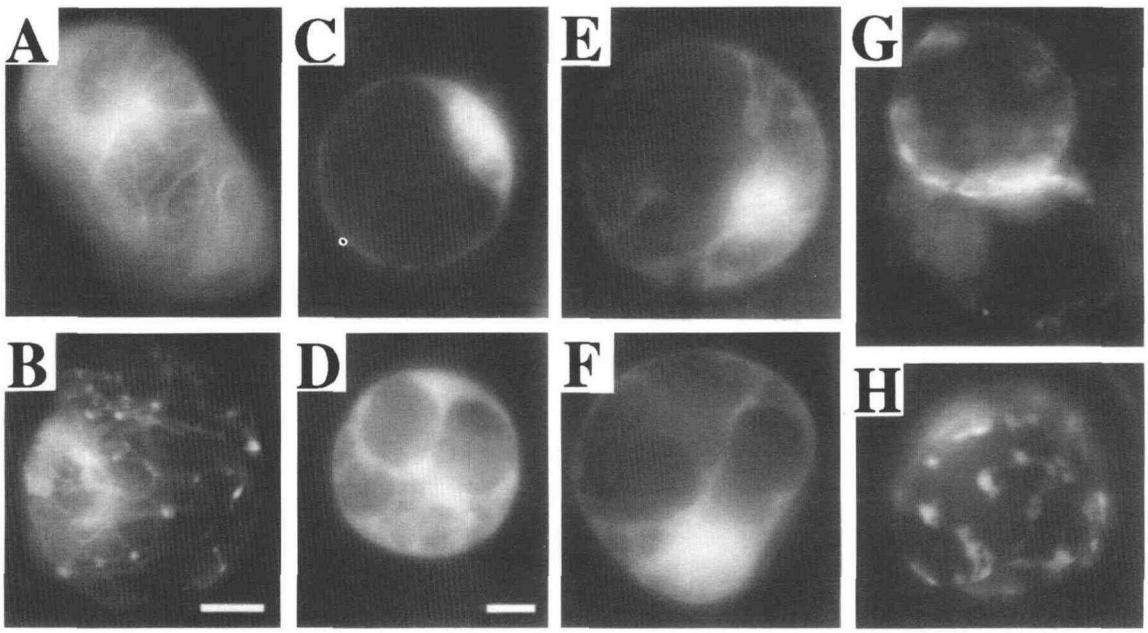

Figure 5. Transient Expression of the P30::GFP Fusion Protein in Tobacco Protoplasts.

A P30::GFP fusion was detected by autofluorescence of GFP.
(A) Expression of the P30::GFP fusion in an unfixed protoplast 18 hr after transfection.
(B) Expression of the P30::GFP fusion in an aldehyde-fixed protoplast 18 hr after transfection.
(C) Expression of GFP alone in an unfixed protoplast 18 hr after transfection.
(D) Expression of GFP alone in an aldehyde-fixed protoplast 18 hr after transfection.
(E) Expression of the GFP::P30 fusion in an unfixed protoplast 18 hr after transfection.
(F) Expression of the GFP::P30 fusion in an aldehyde-fixed protoplast 18 hr after transfection.
(G) Expression of the P30::GFP fusion in unfixed protoplasts 48 hr after transfection.
(H) Expression of the P30::GFP fusion in an aldehyde-fixed protoplast 48 hr after transfection.
Bar in **(B)** = 10 μm for **(A)**, **(B)**, **(E)**, and **(F)**; bar in **(D)** = 10 μm for **(C)**, **(D)**, **(G)**, and **(H)**.

of the P30 filaments colocalized with the rhodamine-phalloidin–labeled actin cytoskeleton (Figures 4A to 4D). Thus, P30 appears to associate with at least two components of the plant cytoskeleton: microtubules and actin filaments. However, the number and extent of P30 filaments that colocalized with actin filaments typically were lower than those seen with P30 filaments and microtubules (Figures 4C and 4D). Occasionally, P30 filaments were observed to colocalize primarily with actin filaments (as shown in Figures 4A and 4B) rather than with microtubules. Since the protoplasts were not synchronized, P30 may have associated primarily with actin during a limited, specific stage in the cell cycle.

To evaluate further the association of P30 with actin filaments, protoplasts were incubated with cytochalasin D to disrupt the actin filaments before fixation (Cooper, 1987). If P30 binds actin filaments, the pattern of P30 localization after cytochalasin D treatment should be different from that seen without treatment. Both rhodamine-phalloidin and actin antibodies were used to check disruption of the actin filaments. Decreases in both the length and number of actin filaments were seen in cytochalasin D–treated protoplasts (Figure 4F). Unlike the extensive depolymerization of microtubules by cold treatment, the actin filaments appeared broken and shortened by cytochalasin. Cytochalasin D–induced changes in the P30 network were less obvious (Figure 4E). Based on observations of large numbers of P30-expressing protoplasts, the number and sometimes the length of the P30 filaments appeared to be slightly decreased by cytochalasin D. A few protoplasts also were found in which cytochalasin D treatment disrupted the majority of P30 filaments (data not shown), correlating with the previous observation that P30 colocalized primarily with actin filaments in a small number of protoplasts. In general, however, when compared with cold-treated protoplasts, most P30 filaments remained intact in cytochalasin D–treated protoplasts. The observation that only a subset of the P30 filaments appears affected by cytochalasin D corresponds to the previous observation that most P30 filaments colocalize with microtubules.

Potential Dynamic Nature of P30 Filaments

Since cytoskeletal elements, such as microtubules, appear to play a role in protein trafficking in animal cells, it is plausible

that the association of P30 with cytoskeletal elements may potentiate transport of P30 to the plasmodesmata. To test this hypothesis and to examine protoplasts during extended periods of P30 expression for possible P30 movement within the cytoplasm, the P30 coding sequence was fused to the N terminus of green fluorescent protein (GFP; Chalfie et al., 1994) in the expression vector pRTL2 to form P30::GFP. Figure 5 shows that, as expected, transient expression of P30::GFP produced a filamentous network in protoplasts (Figures 5A and 5B) similar to that detected with P30 antibodies. Again, as seen with immunocytochemically detected P30, the extent of the P30::GFP network varied from cell to cell. P30::GFP appeared as filamentous arrays, as shown in Figure 5A, but condensed aggregates of P30::GFP interspersed along the filaments were present in some of the protoplasts (Figure 5B). In a few cells, large aggregates could be detected along fine filaments (data not shown). The P30::GFP fusion always displayed more protein aggregates than P30 alone. This result suggests that the addition of GFP to P30 interferes to some extent with filament formation so that P30::GFP aggregates occurred more readily than with wild-type P30. Filaments were not present when control pRTL2::GFP alone was expressed in protoplasts (Figures 5C and 5D), indicating that GFP does not produce the filamentous network. The filamentous appearance of P30::GFP was observed only with P30 fusions to the N terminus of GFP. When P30 was fused to the C terminus of GFP, the intracellular location was typically cytoplasmic (Figures 5E and 5F), resembling the pattern of GFP alone, with fluorescence localizing to cytoplasmic strands (Figures 5C and 5D). Therefore, it is likely that the C-terminal fusions may inactivate P30, possibly by altering P30 conformation or by masking the region of P30 responsible for the formation of the filaments.

The P30::GFP pattern in protoplasts 48 to 72 hr after transfection differed from the pattern seen after 18 to 20 hr. The P30::GFP networks were not as obvious, suggesting that less of the fusion was found as filaments or was associated with cytoskeletal filaments. Most of the P30::GFP at the later time points appeared as aggregates along the periphery of the protoplasts (Figures 5G and 5H). In some aggregating cells, the P30::GFP fusion preferentially accumulated where the cells were in contact (Figure 5G), an area in which secondary plasmodesmata have been reported to form (Monzer, 1991). Thus, the previous positioning of P30 along filaments may represent an earlier stage in the migration of P30 to the exterior of the cell, where, in intact tissue, plasmodesmata may be found.

We next compared the localization pattern of P30 expressed in a steady state versus a transient expression system. For this purpose, protoplasts were isolated from a cell suspension culture originating from leaves of a P30-transformed plant. In leaves of intact transgenic plants, P30 is deposited in the cell wall, specifically in the secondary plasmodesmata (Deom et al., 1990; Ding et al., 1992). Enzymatic digestion of the P30 transgenic cell suspension culture for several hours did not completely remove the cell walls. Consequently, the transgenic "protoplasts" were oblong rather than rounded, as seen with normal protoplasts. Immunocytochemistry of these "protoplasts" revealed that P30 was found predominately around the perimeter near the cell walls, as shown in Figures 6A, 6B, and 6D; P30 was detected in the cross-wall of the protoplast in Figure 6D, suggesting that P30 is deposited in the cell wall in these transgenic cell cultures. P30 filaments were also present in the transgenic cells, as shown in Figure 6C, a different focal plane of the cell from that shown in Figures 6A and 6B.

In Vitro Binding of P30 to Cytoskeletal Proteins

Treatment with both cold and cytochalasin D disrupted the filamentous P30 network, indicating that P30 associates with microtubule and actin filament cytoskeletons. These in vivo studies clearly showed coalignment between microtubules and numerous P30 filaments, but association of actin filaments and

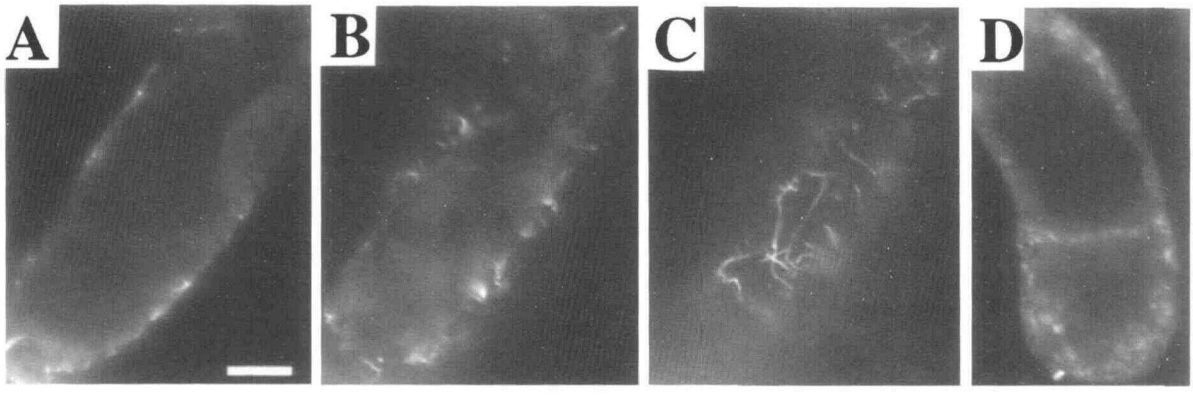

Figure 6. Localization of P30 Near the Cell Periphery and in Filamentous Arrays in P30 Transgenic Cells.

P30 was detected by affinity-purified P30 polyclonal antibody and fluorescein-conjugated goat anti-rabbit secondary antibody.
(A) to **(C)** Different focal planes of P30 in the same aldehyde-fixed P30-transgenic protoplast.
(D) P30 in a different aldehyde-fixed P30-transgenic protoplast.
Bar = 10 μm for **(A)** to **(D)**.

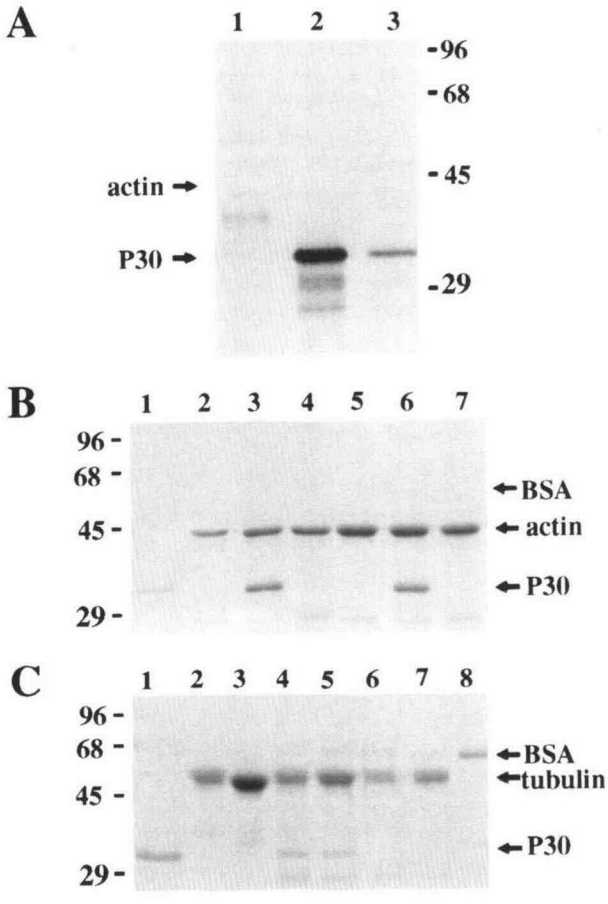

Figure 7. In Vitro Assays of P30 Binding to Actin and Tubulin.

(A) Actin sedimentation assay with in vitro–translated P30 RNA. The autoradiograph of a 10.5% SDS–polyacrylamide protein gel assaying translation products that cosediment with rabbit muscle actin is shown. The positions of actin and P30 (as detected by Coomassie blue staining) are indicated at left, and protein molecular weight markers are indicated at right in kilodaltons. Lane 1 contains the pellet from cosedimentation of actin and translation products when no P30 RNA was added to the translation system; lane 2 contains the pellet from cosedimentation of actin and soluble translation products when P30 RNA was added to the translation system; and lane 3 contains the pellet from centrifugation of P30 translation products. This insoluble material is removed before incubation with polymerized actin.

(B) Analysis of actin and P30 association using magnetic beads. The 10.5% SDS–polyacrylamide protein gel was stained with Coomassie blue to detect actin and proteins that associated with rabbit muscle actin. The positions of actin, P30, and BSA are denoted at right, and the protein molecular weight markers are at left in kilodaltons. Lane 1 contains P30 alone; lane 2, monomeric biotinylated actin with no added P30; lane 3, monomeric biotinylated actin after incubation with P30; lane 4, monomeric biotinylated actin after incubation with BSA; lane 5, polymerized biotinylated actin with no added P30; lane 6, polymerized biotinylated actin after incubation with P30; and lane 7, polymerized biotinylated actin after incubation with BSA.

(C) Analysis of tubulin and P30 association using magnetic beads. The 10.5% SDS–polyacrylamide protein gel was stained with Coomassie blue to detect porcine brain tubulin and associated proteins. The positions of tubulin, P30, and BSA are denoted at right, and the protein molecular weight markers are at left in kilodaltons. Lane 1 contains P30 alone; lane 2, biotinylated tubulin; lane 3, unbiotinylated tubulin; lane 4, polymerized biotinylated tubulin after incubation with P30; lane 5, unpolymerized biotinylated tubulin after incubation with P30; lane 6, polymerized biotinylated tubulin after incubation with BSA; lane 7, polymerized biotinylated tubulin with no added P30; and lane 8, BSA alone.

P30 filaments often was less pronounced. Usually, when compared with that seen with microtubules, the area of colocalization of a single P30 filament with an actin filament was quite limited, and P30 colocalized with actin filaments over short distances only. To test further the interaction of P30 with actin, in vitro binding assays were performed. Since P30 accumulates only transiently in TMV-infected plants, P30 is more readily produced in and purified from *Escherichia coli* for in vitro experiments. However, *E. coli*–produced P30 is often found in inclusion bodies and subsequently exhibits low solubility. The high-speed centrifugation used in typical actin filament sedimentation assays causes P30 alone to sediment. Thus, two alternate experimental approaches were used.

As shown in Figure 7A, the association of P30 and actin was investigated by sedimentation with in vitro–translated P30. Insoluble ^{35}S-P30 represented only a minor component of the translation reactions (Figure 7A, lane 3) and was removed by centrifugation. Then the soluble ^{35}S-P30 was incubated with unlabeled polymerized actin. Figure 7A, lane 2, shows that ^{35}S-P30 cosedimented with actin filaments, suggesting that it binds directly to actin. The negative control, the in vitro translation product of T7 gene 10, did not cosediment with actin (data not shown). In the second method shown in Figure 7B, P30–actin interactions were tested using biotinylated actin and streptavidin-coupled magnetic beads. Biotinylated monomeric actin or polymerized actin (consisting of a mixture of biotinylated and unbiotinylated actin) was incubated with unlabeled P30. Streptavidin-coupled magnetic beads were used to collect the biotinylated actin, followed by incubation in SDS sample buffer to cleave the biotin cross-linker and release actin and any actin-associated proteins. After removing the beads magnetically, the supernatant containing actin and associated proteins was electrophoresed. Centrifugation was not used at any point in this assay, thus avoiding potential cosedimentation of P30 with actin due to low P30 solubility. This method also permitted interactions of P30 with both monomeric and polymerized actin to be tested easily. The results presented in Figure 7B show that P30 was recovered from both monomeric (Figure 7B, lane 3) and filamentous (Figure 7B, lane 6) actin samples. Control experiments with BSA indicated that BSA does not bind either monomeric or filamentous actin (Figure 7B, lanes 4 and 7). The converse experiment using biotinylated P30 and unlabeled actin gave the same result (data not shown). These data suggest that P30 can bind directly to both monomeric and filamentous actin.

From the in vivo data, the coalignment of P30 with microtubules is more widespread and obvious than that of P30 with actin filaments; consequently, the in vitro interaction of P30 with tubulin was not tested as extensively as that of P30 with actin. Nevertheless, in vitro experiments suggest that P30 directly binds tubulin as well as actin. Essentially as described for the experiment testing the association of P30 with actin, shown in Figure 7B, P30–tubulin interactions were assayed using biotinylated tubulin and streptavidin-coupled magnetic beads. The results presented in Figure 7C show that P30 was recovered from both polymerized (Figure 7C, lane 4) and unpolymerized (Figure 7C, lane 5) tubulin samples. Control experiments with BSA indicated that BSA does not bind tubulin (Figure 7C, lane 6). These data suggest that P30 can bind directly to both polymerized and unpolymerized tubulin.

DISCUSSION

The experiments we have presented show that the TMV movement protein P30 forms a filamentous network in the plant cytoplasm that colocalizes with the filamentous arrays of the plant cytoskeleton. Since a P30 mutant, sb-6, did not form this network, the filamentous appearance of wild-type P30 most likely results from a function of P30 rather than its overexpression. The P30 network observed in the present study coincides with random cortical arrays of cytoskeletal filaments in plant protoplasts. As suggested from the pattern of P30 expression, P30 in both transfected and virus-infected protoplasts colocalizes with cytoskeletal filaments, primarily with tubulin and to a lesser extent with actin. Microtubule-depolymerizing treatment disrupted the P30 filamentous pattern, indicating that P30 interacts specifically with microtubules. Disruption of actin filaments by cytochalasin D treatment rarely affected the P30 filamentous pattern, suggesting that the P30 interaction with actin is not as extensive as that with microtubules.

Whether the in vivo interaction of P30 with the plant cytoskeleton occurs directly through P30 or through a cellular protein bound to actin and tubulin is not known. For example, P30 may interact with the cytoskeleton by binding both a microtubule-associated protein and an actin binding protein. Alternatively, P30 may associate indirectly with microtubules via a microtubule-associated protein and directly with actin or vice versa. However, in vitro experiments suggest that P30 can bind directly to both actin and tubulin. Along these lines, another plant viral protein, the 65-kD heat shock protein 70–related protein of beet yellows closterovirus, has been found to bind microtubules in vitro (Karasev et al., 1992). Although P30 appears to bind both actin and tubulin in vitro, the in vivo cellular environment may favor the interaction of P30 with a cytoskeletal-associated component, such as a motor protein, rather than the direct interaction between P30 and tubulin or actin.

The colocalization of P30 filaments with cytoskeletal filaments lends support to the hypothesis that P30 is actively transported through the cytoplasm. P30 along cytoskeletal filaments may be a precursor to localization of P30 to the plasmodesmata and may reflect the association of P30 with a motor protein that shuttles P30 filaments through the cell. That extended expression of P30::GFP resulted in lower amounts of cytoplasmic filamentous P30 and increased amounts of P30 aggregates along the outer edges of the cell suggests that the P30 filamentous localization is transient and may precede P30 movement to the plasma membrane and ultimately to the plasmodesmata. An additional observation supporting this idea is that P30 in protoplasts isolated from transgenic plants is found predominately along the cell wall and plasma membrane and that some P30 is found in a filamentous pattern in the cytoplasm of these protoplasts.

Based on the observed colocalization of P30 with cytoskeletal components and the studies of membrane, organelle, and RNA transport in animals, a model for intracellular transport of P30 can be proposed. In brief, the P30–viral RNA complex could use a "linked" system of microtubules and actin filaments for active transport. This system would be similar to that proposed for squid giant axon organelles in which microtubules are thought to provide tracks for long-distance movement, whereas actin filaments are thought to direct short-distance movement to local sites (Atkinson et al., 1992; Kuznetsov et al., 1992; Langford, 1995). Similarly, both microtubule motor and actin–myosin systems appear to actively transport various mRNAs, as RNA–protein complexes, in animal cells (reviewed in Wilhelm and Vale, 1993). Since viruses tend to exploit cellular mechanisms, the interaction of P30 with both microtubules and actin filaments may mimic transport of the RNA–protein complexes and organelles by using microtubule motors and actin–myosin systems for long- and short-distance transport, respectively (Langford, 1995).

As shown in Figure 8, in the model for P30 intracellular movement, P30 binds to viral RNA to form a P30–viral RNA complex (step 1). We propose from previous evidence (Citovsky et al., 1992a) that the P30–RNA complex is quite elongated and thin. This structure would reduce diffusion within the cytoplasm while favoring organized or directed movement along cytoskeletal elements. According to our model, the cytoskeleton provides a track for the long unfolded P30–RNA complexes and facilitates linear, directed transport. P30 could be associated with the cytoskeleton either before, during, or after RNA complex formation. The P30–RNA complex would first use microtubules for long-distance, possibly bidirectional, movement through the cytoplasm (step 2). Then it would associate with actin filaments for short-distance unidirectional movement to and possibly through plasmodesmata because plasmodesmata appear to contain actin (step 3; White et al., 1994). In addition to the structural actin in plasmodesmata, actin filaments also can be seen extending from both sides of the plasmodesmata into the adjoining cells (White et al., 1994). Thus, P30 is proposed to interact with plasmodesmata-associated actin filaments by using them to target and move through plasmodesmata into the cytoplasm of adjacent cells (step 4). Since TMV P30 itself moves between cells (Waigmann and Zambryski,

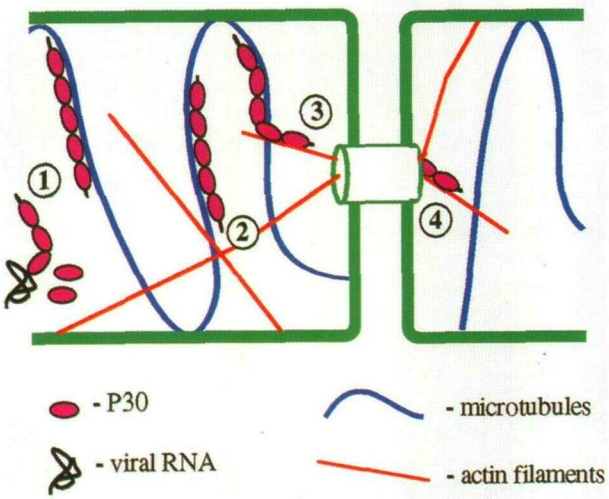

Figure 8. Model for the Movement of the P30–RNA Complex through the Cytoplasm to and through Plasmodesmata.

Step 1 shows that P30 forms a complex, either in the cytoplasm or on the cytoskeleton, with viral RNA. Step 2 shows that the P30–RNA complex moves long distances through the cytoplasm on microtubules, possibly by interacting with a microtubule motor. Step 3 shows that the P30–RNA complex moves short distances to the plasmodesma on plasmodesma-associated actin filaments, possibly via a myosin motor. Step 4 shows that the P30–RNA complex then may move through plasmodesma to adjacent cells on the same plasmodesma-associated actin filaments.

1995), P30 may be shuttled through plasmodesmata by the actin filaments extending between cells. The ability of P30 to increase the plasmodesmal size exclusion limit (Wolf et al., 1989, 1991; Waigmann et al., 1994) may also be related to its interaction with actin, because actin was found in the neck region of plasmodesmata, where the size exclusion limit is thought to be regulated (White et al., 1994).

As suggested by the model, the intracellular association of P30 with both microtubules and actin filaments may facilitate cell-to-cell movement of the P30–RNA complex by providing active transport functions. Further investigations of P30 interaction with the plant cytoskeleton will focus on whether transport occurs by microtubule motors, actin–myosin, or both, and whether cytoskeletal elements play a role in the gating of plasmodesmata by P30. Studies of P30 intracellular transport can act as a model system to analyze the function of plant cytoskeletal elements in intracellular and possibly intercellular transport of proteins and other macromolecular complexes.

METHODS

Plasmid Constructs

The P30 open reading frame was cloned from pETP30 (Citovsky et al., 1990) as an NdeI-BamHI fragment into SmaI-BamHI sites of pGEM7Zf+ (Promega) to form pGEMP30. Before cloning, NdeI was filled in with the Klenow fragment of *Escherichia coli* DNA polymerase. pGEMP30N was constructed using oligonucleotide-directed mutagenesis to insert an NcoI at the start of the P30 coding sequence. pGEMP30N was digested completely with BamHI and digested partially with NcoI to release the entire P30 open reading frame as an 800-bp NcoI-BamHI fragment; this fragment was cloned into the respective sites of pRTL2 (Restrepo et al., 1990) to form pRTLP30.

pRTLP30::GFP contains the entire P30 coding sequence fused in-frame with the coding sequence of green fluorescent protein, GFP (5′ P30 3′::5′ GFP 3′). To construct pRTLP30::GFP, a BspHI site was introduced by oligonucleotide-directed mutagenesis at the termination codon of P30 in pGEMP30N. This changed the P30 termination codon to a methionine, forming pGEMP30NB. pGEMP30NB was digested with BspHI to release a 670-bp fragment that contained the P30 coding sequence from amino acid 43 to the newly added methionine at the end of the coding sequence. To fuse P30 to GFP, the 670-bp BspHI fragment was cloned into the compatible NcoI site of pKSII-GFPN/C (a gift of Drs. J. Roe and G. Peters, University of California, Berkeley, CA), giving pKS-P30::GFP. pKSII-GFPN/C contains a mutagenized version of the GFP gene in pBluescript II KS+ (Stratagene); an NcoI site was engineered at the 5′ of GFP, and the cauliflower mosaic virus (CaMV) 35S polyadenylation signal from pRTL2 was added at the 3′ of the GFP. The fusion between P30 and GFP was cloned from pKS-P30::GFP as a 900-bp ClaI-PstI fragment into the ClaI-PstI sites in pRTLP30, producing the plasmid pRTLP30::GFP. The sequence of pRTLP30::GFP was confirmed by dideoxy sequencing (Sequenase; U.S. Biochemical). As a control for GFP expression, the 850-bp NcoI-PstI fragment from pKSII.GFPN containing the GFP coding sequence plus the CaMV 35S polyadenylation signal was cloned into the respective sites of pRTL2, producing pRTLGFP.

The plasmids pRTLP30, pRTLP30::GFP, and pRTLGFP were used for transient expression of P30, P30::GFP, and GFP, respectively, in protoplasts.

Plant Cell Culture and Electroporation

Suspension cultures of *Nicotiana tabacum* (line XD) were grown in a Murashige and Skoog–based medium, TXD (88 mM sucrose, 1 × Murashige and Skoog salts [GIBCO], 1.3 mg/L niacin, 0.25 mg/L thiamine, 0.25 mg/L pyridoxine, 0.25 mg/L calcium pantothenate, 4 mg/L p-chlorophenoxyacetic acid, 5 mg/L kinetin, 200 mg/L inositol, 130 mg/L asparagine, pH 5.8), and shaken at 200 rpm at 25°C. Protoplasts were prepared according to Howard et al. (1992).

For electroporation, 1 mL of electroporation buffer (10 mM Hepes, pH 7.2, 0.2 M mannitol, 150 mM NaCl, 5 mM $CaCl_2$) was inoculated with 2.5 × 10^6 protoplasts. DNA (50 to 75 μg) was added, and the mixture was placed on ice for 5 to 10 min. Protoplasts were electroporated either at 250 V for a 50-msec pulse in an electroporation apparatus constructed to the specifications described in Fromm et al. (1985) or at 150 V, 500 microfarads in a Bio-Rad electroporator. After electroporation, protoplasts were incubated for 10 min on ice and then for 10 min at room temperature. Protoplasts were diluted to 2.5 × 10^5 protoplasts per mL in TXD medium containing 0.4 M mannitol (TXD-M) and incubated overnight for ~18 to 20 hr at 25°C. Normally, pRTL2 constructs electroporated into protoplasts have transformation efficiencies of 50 to 90% as assayed by protein expression. The efficiency of transformation for pRTL2::P30, however, was typically 20 to 40%, suggesting that expression of P30 is deleterious to the cell.

Virus Infection of Protoplasts

Protoplasts were prepared from *N. tabacum* (line XD) suspension cell culture according to Howard et al. (1992) and inoculated with TMV using polyethylene glycol as described by Maule et al. (1980). Inoculated protoplasts were cultured in TXD medium under continual light at 25°C and assayed immunocytochemically for P30 expression after 10 hr.

Transgenic Cell Suspension Cultures

A transgenic tobacco line expressing P30, produced as described in Citovsky et al. (1992b), was grown under sterile conditions. Leaves were removed from the plants, cut from the midrib to the margin with a scalpel every 3 to 4 mm, and incubated in 1% cellulase, 0.1% macerozyme in K3+ (10 mM $CaCl_2$, 0.45 M sucrose, 1 × Murashige and Skoog salts [GIBCO], 1.3 mg/L niacin, 10.25 mg/L thiamine, 1.25 mg/L pyridoxine, 0.25 mg/L calcium pantothenate, 0.1 mg/L 2,4-dichlorophenoxyacetic acid, 0.2 mg/L 6-benzylaminopurine, 1 mg/L naphthaleneacetic acid, 250 mg/L xylose, 100 mg/L myoinositol, 1 mg/L nicotinic acid, pH 5.8) overnight at 25°C with gentle shaking. The undigested leaf tissue and veins were removed and the remaining solution centrifuged at 100 to 150*g* for 5 min to collect protoplasts. The protoplasts were washed twice with K3+ and then cultured in K3+ at 25°C without shaking. The high osmolarity concentration was gradually reduced by diluting K3+ with TXD every 7 days. After 7 weeks, cultures were gently shaken to facilitate growth and then at 10 weeks were maintained at 25°C and shaken at 200 rpm. After 12 to 15 weeks, the cell suspension culture was used for protoplasts as described above.

Immunocytochemistry and GFP Fusion Protein Expression

The P30 protein was purified from *E. coli* as described by Citovsky et al. (1990) and used for production of polyclonal antibodies in rabbits. Specific P30 antibodies were purified from the rabbit antisera by affinity for the P30 protein immobilized on polyvinylidene difluoride membrane (Immobilon P; Millipore, Bedford, MA; Smith and Fisher, 1984).

Before immunocytochemistry with P30 antibodies, protoplasts were either aldehyde fixed or detergent permeabilized (Kengen and de Graaf, 1991; Kengen and Derksen, 1991). For fixation, protoplasts were incubated for 0.5 to 1 hr in 3 to 4% formaldehyde (freshly prepared from paraformaldehyde), 10 mM EGTA, 5 mM $MgSO_4$, 1 mM phenylmethylsulfonyl fluoride, 2 μg/mL aprotinin, 2 μg/mL leupeptin, 1 μg/mL pepstatin, and 10% DMSO in 100 mM Pipes, pH 6.9, and then rinsed for 10 min in 100 mM Pipes, pH 6.9. For detergent permeabilization, protoplasts were incubated at room temperature for 30 min in 100 mM Pipes, pH 6.9, 10% DMSO, 10 mM EGTA, 5 mM $MgSO_4$, 0.05% Nonidet P-40 (v/v), and 0.4 M mannitol.

The following procedure was used with both aldehyde-fixed and detergent-permeabilized protoplasts. For P30-microtubule studies, protoplasts were incubated for 1 hr at room temperature with P30 affinity-purified polyclonal rabbit antibody and tubulin mouse monoclonal antibody. Protoplasts were washed with a large volume of PBS (10 mM phosphate, pH 7.4, 150 mM NaCl) to remove primary antibodies and then incubated for 30 min at room temperature with fluorescein-conjugated goat anti-rabbit IgG (Calbiochem; diluted 1:30 in PBS) and rhodamine-conjugated goat anti-mouse IgG (Calbiochem; diluted 1:30 in PBS). Following incubations with secondary antibodies, protoplasts again were washed with a large volume of PBS. To prevent fading of the fluorescent signal, protoplasts were resuspended in Citifluor PBS–Citifluor glycerol (Ted Pella, Inc., Redding, CA; combined 1:2).

For P30–actin studies, protoplasts were treated as described above except that P30 affinity-purified polyclonal rabbit antibody was used in primary antibody incubations and fluorescein-conjugated goat anti-rabbit IgG (Calbiochem; diluted 1:30 in PBS) and 0.33 to 0.66 μM rhodamine phalloidin (Molecular Probes, Eugene, OR) were used in secondary antibody incubations.

During some experiments, protoplasts were treated with either cold or cytochalasin D before fixation. For cold treatment, 5×10^5 protoplasts were incubated at 0°C for 0.5 to 1 hr and then aldehyde fixed. For cytochalasin D treatment, 5×10^5 protoplasts were incubated with 50 to 100 μM cytochalasin D for 0.5 to 1 hr at room temperature. Protoplasts were washed briefly with TXD-M and then aldehyde fixed.

For P30::GFP fusions, protoplasts were either observed directly without fixation or briefly aldehyde fixed. For fixation, protoplasts were incubated for 10 to 15 min in 3 to 4% formaldehyde (freshly prepared from paraformaldehyde), 10 mM EGTA, 5 mM $MgSO_4$, and 10% DMSO in 100 mM Pipes, pH 6.9. Protoplasts were rinsed for 10 min in 100 mM Pipes, pH 6.9, and then briefly rinsed with PBS.

Observations were performed on a Zeiss Axiophot epifluorescence microscope (Carl Zeiss, Inc., Thornwood, NY). Images were captured with a cooled CCD (model TEA/CCD-1400TK; Princeton Instruments, Inc., Trenton, NJ) controlled by IPLab (Signal Analytics, Vienna, VA). Digital images were processed and figures assembled using Adobe Photoshop (Adobe Systems, Mountain View, CA).

P30:Actin Cosedimentation Assay

As a template for in vitro transcription, pGEMP30 was linearized with BamHI. Messenger P30 RNA was transcribed from the template using T7 DNA polymerase (New England Biolabs, Beverly, MA) and 7-methylguanosine cap (Pharmacia Biotechnology) as described in Promega Protocols and Application Guide. The P30 RNA was translated in a wheat germ translation system (Promega); a typical 50-μL translation reaction contained 25 μL wheat germ extract, 10 μCi ^{35}S-methionine (Amersham), and ~1 to 2 μg RNA from the transcription reaction. The reaction was incubated at 25°C for 1 hr. Labeled translation products were resolved by 12.5% SDS-PAGE and detected by fluorography.

Before cosedimentation assays, 1 μL of the translation reaction was diluted with 99 μL of F buffer (50 mM Hepes, pH 7.5, 0.2 mM $CaCl_2$, 0.1 M KCl, 5 mM $MgCl_2$, and 1 mM ATP) and then centrifuged for 10 min at 80,000*g* to sediment insoluble proteins. Immediately following centrifugation, aliquots of the translation reaction were used for actin cosedimentation assays. Rabbit or chick muscle actin was polymerized by adjusting buffer conditions from G buffer (50 mM Hepes, pH 7.5, 0.2 mM $CaCl_2$, 0.2 mM ATP) to that of F buffer. Cosedimentation assays then were performed by mixing 25 μL of in vitro translation products with 5 to 15 μg of polymerized actin. The mixture was incubated at room temperature or on ice for 1 hr and then centrifuged for 10 min at 80,000*g* either directly or layered over a cushion of 10% sucrose in F buffer. After removal of the supernatant, the pellet was washed with F buffer and solubilized with sample buffer. The pellet and supernatant fractions were electrophoresed by 10.5% SDS-PAGE. Actin was detected by Coomassie Brilliant Blue R 250 staining, and cosedimenting translation products were detected by fluorography.

Magnetic Assay for P30:Actin and P30:Tubulin Interactions

Rabbit muscle actin (3 to 4 mg) was labeled with biotin-HPDP as directed by the manufacturer (Pierce, Rockford, IL). Uncoupled biotin-HPDP was removed over a desalting column (Bio-Gel P; Bio-Rad), and biotinylated actin was stored in G buffer. Linkage of biotin to actin was confirmed by dot blot. Presumptive biotinylated actin was absorbed to Immobilon P in a dot blot filtering apparatus. The filter was removed, blocked for 1 hr at room temperature with 5% BSA-TBS (50 mM Tris, 200 mM NaCl, pH 7.4), and incubated for 30 min at room temperature with streptavidin–alkaline phosphatase conjugate diluted 1:5000 in 1% BSA-TBS. After extensive washing, the blot was developed using nitro blue tetrazolium and 5-bromo-4-chloro-3-indolyl phosphate. As determined by sedimentation assays, biotinylation of actin did not appear to affect polymerization significantly.

For actin binding assays, biotinylated actin was polymerized by adding 1 μg native actin per 2 μg biotinylated actin and adjusting buffer conditions to that of F buffer. Either monomeric biotinylated or polymerized biotinylated actin (1.5 μg) was incubated at room temperature for 20 to 30 min with 0.2 to 0.4 μg P30 purified from *E. coli* (Citovsky et al., 1990) or, as a negative control, with 0.4 μg BSA. Streptavidin paramagnetic beads (5 to 7 μg; Promega; protein/antibody qualified) were incubated with the actin–P30 mixture at room temperature for 15 min. The beads were magnetically attracted to the side of the microcentrifuge tube, allowing the supernatant to be removed. The beads were washed two to three times by 5- to 10-min incubations at room temperature with gentle shaking. The washes were removed by again magnetically attracting the beads to the side of the microcentrifuge tube. Washes were performed in either G buffer for the monomeric actin–P30 mixture or F buffer for the polymerized actin–P30 mixture. The biotinylated actin and any actin-associated protein were released from the biotin by incubating the beads in SDS sample buffer 5 to 10 min at 55°C to cleave the biotin cross-linker. The beads again were magnetically attached to the side of the microcentrifuge tube, allowing removal of the supernatant containing the actin and associated protein in sample buffer. The supernatant was electrophoresed by 10.5% SDS-PAGE and analyzed by Coomassie blue staining.

For tubulin binding assays, biotin-porcine brain tubulin (Cytoskeleton, Denver, CO) was polymerized at a concentration of 1 to 3 μg/μL in G-PEM-1 (80 mM Pipes, pH 6.8, 1 mM $MgSO_4$, 1 mM EGTA, 1 mM GTP) plus 10 to 15% glycerol (v/v) for 30 min at 35°C. Either unpolymerized or polymerized biotinylated tubulin (3 μg) was incubated at room temperature for 20 to 30 min with 0.2 to 0.4 μg P30 purified from *E. coli* (Citovsky et al., 1990) or, as a negative control, with 0.4 μg BSA. Streptavidin paramagnetic beads (5 to 7 μg; Promega; protein/antibody qualified) were incubated with the tubulin–P30 mixture at room temperature for 15 min. The beads were magnetically attracted to the side of the microcentrifuge tube, allowing the supernatant to be removed. The beads were washed two to three times by 5- to 10-min incubations at room temperature with gentle shaking. The washes were removed by again magnetically attracting the beads to the side of the microcentrifuge tube. Washes were done in either G-PEM-0.1 (80 mM Pipes, pH 6.8, 1 mM $MgSO_4$, 1 mM EGTA, 0.1 mM GTP) for the unpolymerized tubulin–P30 mixture or G-PEM-1 plus glycerol for the polymerized tubulin–P30 mixture. Unlike the linkage between actin and biotin, the linkage between tubulin and biotin was not cleavable. Thus, the biotinylated tubulin and any tubulin-associated protein were released from the beads by boiling the beads in SDS sample buffer for 10 min. The beads again were magnetically attached to the side of the microcentrifuge tube, allowing removal of the supernatant containing the tubulin and associated protein in sample buffer. The supernatant was electrophoresed by 10.5% SDS-PAGE and analyzed by Coomassie blue staining.

ACKNOWLEDGMENTS

We thank Dan Oppenheimer and Dr. Ted Wong for rabbit and chick actin, the laboratory of Dr. Zac Cande for the tubulin antibody, Drs. Judith Roe and Gary Peters for pKSII.GFPN/C, and Dr. Steve Ruzin and Hans E.E. Holtan for their invaluable help with imaging and microscopy. We thank Dr. Vitaly Citovsky and Dr. Andy Jackson for critical reading of this manuscript and for encouragement. We gratefully acknowledge members of the Zambryski laboratory for many helpful discussions. This work was supported by National Institutes of Health Grant No. GM45244 awarded to P.C.Z.

Received July 31, 1995; accepted October 4, 1995.

REFERENCES

Atkinson, S.J., Doberstein, S.K., and Pollard, T.D. (1992). Moving off the beaten tracks. Curr. Biol. **2,** 326–328.

Bassell, G.J., Taneja, K.L., Kislauskis, E.H., Sundell, C.L., Posers, C.M., Ross, A., and Singer, R.H. (1994). Actin filaments and the spatial positioning of mRNAs. In Actin: Biophysics, Biochemistry and Cell Biology, J.E. Estes and P.J. Higgins, eds (New York: Plenum Press), pp. 183–189.

Blum, H., Gross, H.J., and Beier, H. (1989). The expression of the TMV-specific 30-kDa protein in tobacco protoplasts is strongly and selectively enhanced by actinomycin. Virology **169,** 51–61.

Chalfie, M., Tu, Y., Euskirchen, G., Ward, W.W., and Prasher, D.C. (1994). Green fluorescent protein as a marker for gene expression. Science **263,** 802–805.

Citovsky, V. (1993). Probing plasmodesmal transport with plant viruses. Plant Physiol. **102,** 1071–1076.

Citovsky, V., and Zambryski, P. (1991). How do plant virus nucleic acids move through intercellular connections? BioEssays **13,** 373–379.

Citovsky, V., and Zambryski, P. (1993). Transport of nucleic acids through membrane channels: Snaking through small holes. Annu. Rev. Microbiol. **47,** 167–197.

Citovsky, V., Knorr, D., Schuster, G., and Zambryski, P. (1990). The P30 movement protein of tobacco mosaic virus is a single strand nucleic acid binding protein. Cell **60,** 637–647.

Citovsky, V., Wong, M.L., Shaw, A.L., Prasad, B.V.V., and Zambryski, P. (1992a). Visualization and characterization of tobacco mosaic virus movement protein binding to single-stranded nucleic acids. Plant Cell **4,** 397–411.

Citovsky, V., Zupan, J., Warnick, D., and Zambryski, P. (1992b). Nuclear localization of Agrobacterium VirE2 protein in plant cells. Science **256,** 1803–1805.

Citovsky, V., McLean, B.G., Zupan, J.R., and Zambryski, P. (1993). Phosphorylation of tobacco mosaic virus cell-to-cell movement protein by a developmentally regulated plant cell wall–associated protein kinase. Genes Dev. **7,** 904–910.

Cooper, J.A. (1987). Effects of cytochalasin and phalloidin on actin. J. Cell Biol. **105,** 1473–1478.

Deom, C.M., Shaw, M.J., and Beachy, R.N. (1987). The 30-kilodalton gene product of tobacco mosaic virus potentiates virus movement. Science **327,** 389–394.

Deom, C.M., Schubert, K.R., Wolf, S., Holt, C.A., Lucas, W.J., and Beachy, R.N. (1990). Molecular characterization and biological function of the movement protein of tobacco mosaic virus in transgenic plants. Proc. Natl. Acad. Sci. USA **87,** 3284–3288.

Deom, C.M., Lapidot, M., and Beachy, R.N. (1992). Plant virus movement proteins. Cell **69,** 221–224.

Ding, B., Haudsenshield, J.S., Hull, R.J., Wolf, S., Beachy, R.N., and Lucas, W.J. (1992). Secondary plasmodesmata are specific sites of localization of the tobacco mosaic virus movement protein in transgenic tobacco plants. Plant Cell **4,** 915–928.

Dingwall, C. (1992). Soluble factors and solid phases. Curr. Biol. **2,** 503–505.

Fromm, M., Taylor, L.P., and Walbot, V. (1985). Expression of genes transferred into monocot and dicot plant cells by electroporation. Proc. Natl. Acad. Sci. USA **82,** 5822–5828.

Gibbs, A.J. (1976). Viruses and plasmodesmata. In Intercellular Communication in Plants: Studies on Plasmodesmata, B.E.S. Gunning and A.W. Robards, eds (Berlin: Springer-Verlag), pp. 149–164.

Haseloff, J., Goelet, P., Zimmern, D., Ahlquist, P., Dasgupta, R., and Kaesberg, P. (1984). Striking similarities in amino acid sequence among nonstructural proteins encoded by RNA viruses that have dissimilar genomic organization. Proc. Natl. Acad. Sci. USA **81,** 4358–4362.

Hesketh, J. (1994). Translation and the cytoskeleton: A mechanism for targeted protein synthesis. Mol. Biol. Rep. **19,** 233–243.

Howard, E.A., Zupan, J.R., Citovsky, V., and Zambryski, P. (1992). The VirD2 protein of *A. tumefaciens* contains a C-terminal bipartite nuclear localization signal: Implications for nuclear uptake of DNA in plant cells. Cell **68,** 109–118.

Karasev, A.V., Kashina, A.S., Gelfand, V.I., and Dolja, V.V. (1992). HSP70-related 65 kDa protein of beet yellows closterovirus is a microtubule-binding protein. FEBS Lett. **304,** 12–14.

Kengen, H.M.P., and de Graaf, B.H. (1991). Microtubules and actin filaments co-localize extensively in non-fixed cells of tobacco. Protoplasma **163,** 62–65.

Kengen, H.M.P., and Derksen, J. (1991). Organization of microtubules and microfilaments in protoplasts from suspension cells of *Nicotiana plumbaginifolia*: A quantitative analysis. Acta Bot. Neerl. **40,** 29–40.

Kiberstis, P.A., Pessi, A., Atherton, E., Joacson, R., Hunter, T., and Zimmern, D. (1983). Analysis of in vitro and in vivo products of the TMV 30 kDa open reading frame using antisera raised against a synthetic peptide. FEBS Lett. **164,** 355–360.

Koonin, E.V., and Dolja, V.V. (1993). Evolution and taxonomy of positive-strand RNA viruses: Implications of comparative analysis of amino acid sequences. Crit. Rev. Biochem. Mol. Biol. **28,** 375–430. Erratum. Crit. Rev. Biochem. Mol. Biol. **28,** 546.

Kuznetsov, S.A., Langford, G.M., and Weiss, D.G. (1992). Actin-dependent organelle movement in squid axoplasm. Nature **356,** 722–725.

Langford, G.M. (1995). Actin- and microtubule-dependent organelle motors: Interrelationships between the two motility systems. Curr. Opin. Cell Biol. **7,** 82–88.

Lehto, K., Bubrick, P., and Dawson, W.O. (1990). Time course of TMV 30K protein accumulation in intact leaves. Virology **174,** 290–293.

Lloyd, C.W. (1982). The Cytoskeleton in Plant Growth and Development. (New York: Academic Press).

Luby-Phelps, K. (1993). Effect of cytoarchitecture on the transport and localization of protein synthetic machinery. J. Cell. Biochem. **52,** 140–147.

Luby-Phelps, K. (1994). Physical properties of cytoplasm. Curr. Opin. Cell Biol. **6,** 3–9.

Lucas, W.J., and Gilbertson, R.L. (1994). Plasmodesmata in relation to viral movement within leaf tissues. Annu. Rev. Phytopathol. **32,** 387–411.

Maule, A.J., Boulton, M.I., Edmunds, C., and Wood, K.R. (1980). Polyethylene glycol–mediated infection of cucumber protoplasts by cucumber mosaic virus and virus RNA. J. Gen. Virol. **47,** 199–203.

McLean, B.G., Waigmann, E., Citovsky, V., and Zambryski, P. (1993). Cell-to-cell movement of plant viruses. Trends Microbiol. **1,** 105–109.

Melki, R., Gaudin, Y., and Blondel, D. (1994). Interaction between tubulin and the viral matrix protein of vesicular stomatitis virus: Possible implications in the viral cytopathic effect. Virology **202,** 339–347.

Meshi, T., Watanabe, Y., Saito, T., Sugimoto, A., Maeda, T., and Okada, Y. (1987). Function of the 30 kD protein of tobacco mosaic virus: Involvement in cell-to-cell movement and dispensability for replication. EMBO J. **6,** 2557–2563.

Meshi, T., Hosokawa, D., Kawagishi, M., Watanabe, Y., and Okada, Y. (1992). Reinvestigation of intracellular localization of the 30K protein in tobacco protoplasts infected with tobacco mosaic virus RNA. Virology **187,** 809–813.

Monzer, J. (1991). Ultrastructure of secondary plasmodesmata formation in regenerating *Solanum nigrum*–protoplast cultures. Protoplasma **165,** 86–95.

Morozov, S., Dolja, V.V., and Atabekov, J.G. (1989). Probable reassortment of genomic elements among elongated RNA-containing plant viruses. J. Mol. Evol. **29,** 52–62.

Moser, O., Gagey, M.-J., Godefroy-Colburn, T., Stussi-Garaud, C., Ellwart-Tscurtz, M., Nitschko, H., and Mundry, K.-W. (1988). The fate of the transport protein of tobacco mosaic virus in systemic and hypersensitive tobacco hosts. J. Gen. Virol. **69,** 1367–1373.

Pasick, J.M., Kalicharran, K., and Dales, S. (1994). Distribution and trafficking of JHM coronavirus structural proteins and virions in primary neurons and the OBL-21 neuronal cell line. J. Virol. **68,** 2915–2928.

Restrepo, M.A., Freed, D.D., and Carrington, J.C. (1990). Nuclear transport of plant potyviral proteins. Plant Cell **2,** 987–998.

Shibaoka, H., and Nagai, R. (1994). The plant cytoskeleton. Curr. Opin. Cell Biol. **6,** 10–15.

Singer, R. (1992). The cytoskeleton and mRNA localization. Curr. Opin. Cell Biol. **4,** 15–19.

Smith, D.E., and Fisher, P.A. (1984). Identification, developmental regulation, and response to heat shock of two antigenically related forms of a major nuclear envelope protein in *Drosophila* embryos: Application of an improved method for affinity purification of antibodies using polypeptides immobilized on nitrocellulose blots. J. Cell Biol. **99,** 20–28.

Staiger, C.J., and Lloyd, C.W. (1991). The plant cytoskeleton. Curr. Opin. Cell Biol. **3,** 33–42.

Topp, K.S., Meade, L.B., and LaVail, J.H. (1994). Microtubule polarity in the peripheral processes of trigeminal ganglion cells: Relevance for the retrograde transport of herpes simplex virus. J. Neurosci. **14,** 318–325.

Vale, R.D. (1987). Intracellular transport using microtubule-based motors. Annu. Rev. Cell Biol. **3,** 347–378.

Waigmann, E., and Zambryski, P. (1995). Tobacco Mosaic Virus movement protein–mediated protein transport between trichome cells. Plant Cell **7,** 2069–2079.

Waigmann, E., Lucas, W.J., Citovsky, V., and Zambryski, P. (1994). Direct functional assay for tobacco mosaic virus cell-to-cell movement protein and identification of a domain involved in increasing plasmodesmal permeability. Proc. Natl. Acad. Sci. USA **91,** 1433–1437.

Watanabe, Y., Emori, Y., Ooshika, I., Meshi, T., Ohno, T., and Okada, Y. (1984). Synthesis of TMV-specific RNAs and proteins at the early stage of infection in tobacco protoplasts: Transient expression of the 30K protein and its mRNA. Virology **133,** 18–24.

White, R.G., Badelt, K., Overall, R.L., and Vesk, M. (1994). Actin associated with plasmodesmata. Protoplasma **180,** 169–184.

Wilhelm, J.E., and Vale, R.D. (1993). RNA on the move: The mRNA localization pathway. J. Cell Biol. **123,** 269–274.

Williamson, R. (1986). Organelle movements along actin filaments and microtubules. Plant Physiol. **82,** 631–634.

Wolf, S., Deom, C.M., Beachy, R.N., and Lucas, W.J. (1989). Movement protein of tobacco mosaic virus modifies plasmodesmatal size exclusion limit. Science **246,** 377–379.

Wolf, S., Deom, C.M., Beachy, R., and Lucas, W.J. (1991). Plasmodesmatal function is probed using transgenic tobacco plants that express a virus movement protein. Plant Cell **3,** 593–604.

Zimmern, D. (1988). Evolution of RNA viruses. In RNA Genetics, J. Holland, E. Domingo, and P. Ahlquist, eds (Boca Raton, FL: CRC Press), pp. 211–240.